Title

Macrophage Migration Inhibitory Factor as a Chaperone Inhibiting Accumulation of Misfolded SOD1

Journal

Neuron, 86(1)

ISSN

0896-6273

Authors

Israelson, Adrian
Ditsworth, Dara
Sun, Shuying
et al.

Publication Date

2015-04-01

DOI

10.1016/j.neuron.2015.02.034

Peer reviewed

HHS Public Access

Author manuscript

Neuron. Author manuscript; available in PMC 2016 April 08.

Published in final edited form as:

Neuron. 2015 April 8; 86(1): 218–232. doi:10.1016/j.neuron.2015.02.034.

Macrophage Migration Inhibitory Factor (MIF) as a Chaperone Inhibiting Accumulation of Misfolded SOD1

Adrian Israelson[1,#], **Dara Ditsworth**[2,3], **Shuying Sun**[2,3], **SungWon Song**[6,7], **Jason Liang**[2], **Marian Hruska-Plochan**[4], **Melissa McAlonis-Downes**[2], **Salah Abu-Hamad**[1], **Guy Zoltsman**[1], **Tom Shani**[1], **Marcus Maldonado**[2], **Anh Bui**[2], **Michael Navarro**[4], **Huilin Zhou**[2,3], **Martin Marsala**[4], **Brian K. Kaspar**[6,7,8], **Sandrine Da Cruz**[2], and **Don W. Cleveland**[2,3,5,#]

[1]Department of Physiology and Cell Biology, Faculty of Health Sciences and The Zlotowski Center for Neuroscience, Ben-Gurion University of the Negev, P.O.B. 653 Beer Sheva, 84105, Israel

[2]Ludwig Institute for Cancer Research, University of California at San Diego, La Jolla, CA 92093-0670

[3]Department of Cellular and Molecular Medicine, University of California at San Diego, La Jolla, CA 92093-0670

[4]Department of Anesthesiology, University of California at San Diego, La Jolla, CA 92093-0670

[5]Department of Neuroscience, University of California at San Diego, La Jolla, CA 92093-0670

[6]The Research Institute at Nationwide Children's Hospital, The Ohio State University, Columbus OH 43205

[7]Molecular, Cellular and Developmental Graduate Program, The Ohio State University, Columbus OH 43205

[8]Department of Neuroscience, The Ohio State University, Columbus OH 43205

Summary

Mutations in superoxide dismutase (SOD1) cause amyotrophic lateral sclerosis (ALS), a neurodegenerative disease characterized by loss of motor neurons and accompanied by accumulation of misfolded SOD1 onto the cytoplasmic faces of intracellular organelles, including mitochondria and endoplasmic reticulum (ER). Using inhibition of misfolded SOD1 deposition onto mitochondria as an assay, a chaperone activity abundant in non-neuronal tissues is now purified and identified to be the multifunctional macrophage migration inhibitory factor (MIF), whose activities include an ATP-independent protein folding chaperone. Purified MIF is shown to directly inhibit mutant SOD1 misfolding. Elevating MIF in neuronal cells suppresses

[#]Corresponding authors: Prof. Don W. Cleveland, Ludwig Institute for Cancer Research, Univ. of California, San Diego, dcleveland@ucsd.edu; Dr. Adrian Israelson, Dept. of Physiology and Cell Biology, Faculty of Health Sciences, Ben-Gurion University of the Negev, adriani@bgu.ac.il.

accumulation of misfolded SOD1 and its association with mitochondria and ER and extends survival of mutant SOD1-expressing motor neurons. Accumulated MIF protein is identified to be low in motor neurons, implicating correspondingly low chaperone activity as a component of vulnerability to mutant SOD1 misfolding and supporting therapies to enhance intracellular MIF chaperone activity.

Introduction

Amyotrophic lateral sclerosis (ALS) is a progressive adult-onset neurodegenerative disorder characterized by the selective loss of upper and lower motor neurons. About 10% are inherited in a dominant manner (Da Cruz and Cleveland, 2011), with 20% of familial cases caused by mutation cytoplasmic Cu/Zn superoxide dismutase (SOD1) (Rosen et al., 1993). The exact mechanism(s) responsible for motor neuron degeneration remains unsettled, albeit models for each of the nine most prominently proposed pathways include damage from misfolded, mutant SOD1 (Ilieva et al., 2009).

Multiple groups have identified that SOD1 mutants with divergent biochemical characteristics share a common property with a proportion of the predominantly cytosolic SOD1 being localized to mitochondria (Israelson et al., 2010; Liu et al., 2004; Mattiazzi et al., 2002; Vande Velde et al., 2008) and/or endoplasmic reticulum (ER) (Fujisawa et al., 2012; Nishitoh et al., 2008), but only in nervous system tissues in patients samples and rodent models. In particular, misfolded mutant SOD1 association with derlin-1, a component of the endoplasmic reticulum-associated degradation (ERAD) pathway, has been implicated in induction of ER stress from disrupted removal of misfolded proteins from the ER (Fujisawa et al., 2012; Nishitoh et al., 2008). Derlin-1 is bound by at least 132 of the ALS-linked SOD1 mutants, each of which exposes a derlin-1 binding domain buried in correctly folded SOD1 (Fujisawa et al., 2012).

Purification of mitochondria, including floatation steps that eliminate protein only aggregates, has demonstrated mutant SOD1 deposition occurs on the cytoplasmic face of the outer membrane of spinal cord mitochondria (Liu et al., 2004; Vande Velde et al., 2008), accompanied by altered mitochondrial shape and distribution (Vande Velde et al., 2011). These findings were reinforced by demonstration (using sensitivity to proteolysis and immunoprecipitation with an antibody specific for misfolded SOD1) that misfolded forms of both dismutase active and inactive mutant SOD1 are deposited onto the cytoplasmic face of the outer membrane of spinal cord mitochondria (Vande Velde et al., 2008). One component directly bound by misfolded SOD1 is the voltage-dependent anion channel-1 (VDAC1), with binding inhibiting its conductance of adenine nucleotides across the outer mitochondrial membrane (Israelson et al., 2010). Moreover, mutant SOD1 may also interact with other components of the mitochondrial outer membrane including Bcl-2 (Pedrini et al., 2010) and the protein import machinery (Li et al., 2010), thereby altering the corresponding activities.

Recognizing that expression of SOD1 is ubiquitous, but misfolded SOD1 accumulation and binding to mitochondria and the ER is found only in nervous system tissues, one of the most important unsolved questions is the molecular mechanism(s) underlying cell type selectivity

for accumulation of misfolded SOD1 and its association with intracellular organelles. Here we purify a cytosolic activity whose action inhibits mutant SOD1 misfolding onto mitochondria and ER. We identify this factor to be macrophage migration inhibitory factor (MIF), a multifunctional protein whose activities include an ATP-independent protein folding chaperone (Cherepkova et al., 2006). We propose that a low MIF level within motor neurons is one component of their selective vulnerability to ubiquitously expressed mutations in SOD1.

Results

The cytosol determines mutant SOD1 association with mitochondria and ER

We previously reported that ALS-causing mutant SOD1 association with mitochondria was characterized by misfolded SOD1 binding to components, including VDAC1, on the outer mitochondrial membrane, but was found for mitochondria isolated from spinal cord, but not for those similarly purified from liver (Israelson et al., 2010). Consistent with this and other reports, immunoblot analysis of microsomes or mitochondria isolated from spinal cord homogenates (see schematic in Figure 1A) from rats expressing either of two ALS-linked mutations in SOD1 ($SOD1^{G93A}$ (Howland et al., 2002) and $SOD1^{H46R}$ (Nagai et al., 2001)) revealed that mutant SOD1 bound both to microsomal and mitochondrial membranes (Figure 1B). To determine whether this selective association of mutant SOD1 with spinal mitochondria was mediated by the spinal cord mitochondria or the corresponding cytosol, we isolated normal, non-transgenic mitochondria from spinal cord and liver. Those mitochondria were then incubated (Figure 1C) with cytosolic extracts prepared (as in Figure 1A) from spinal cords or livers of rats expressing dismutase active ($SOD1^{G93A}$) or inactive ($SOD1^{H46R}$) mutants.

The mitochondria were re-isolated and analyzed by immunoblotting for mutant SOD1. Although the liver and spinal cord cytosols contained comparable levels of mutant human SOD1 (Figure 1C, bottom), none of the mutant SOD1 in liver cytosol bound to liver or spinal cord derived, non-transgenic mitochondria. In contrast, incubation with spinal cord cytosols from $SOD1^{G93A}$ or $SOD1^{H46R}$ expressing rats did yield association of a proportion of both mutant SOD1s with wild type mitochondria. For both dismutase active ($SOD1^{G93A}$) and inactive ($SOD1^{H46R}$) mutants, binding was independent of the tissue from which the mitochondria were isolated (Figure 1C). Thus, the tissue origin of the cytosol, not of the mitochondrion, determines whether mutant SOD1 in those cytosols binds to mitochondria.

Next, we investigated if there was a factor(s) in spinal cord cytosol that induced association of SOD1 with normal mitochondria, or in contrast, if some factor in the liver prevented binding. To do this, recombinant $SOD1^{G85R}$ was incubated with mitochondria purified from liver of non-transgenic rats in the presence of $SOD1^{G93A}$ spinal cord or liver extract. While spinal cord cytosol did not affect $SOD1^{G85R}$ association with mitochondria (Figure 1D, lane 5), added liver cytosol inhibited it (Figure 1D, compare lanes 1 and 2). This inhibitory activity was not affected by inhibitors of the Hsp70 and Hsp90 protein chaperones and was independent of calcium (Figure S1). Remarkably, although the inhibitory activity was heat labile (consistent with a protein activity), it was not inactivated by degradation of most proteins by incubation of the liver cytosol with proteinase K (Figure 1D, lane 3).

Identification of MIF as an inhibitor of mutant SOD1 association with mitochondria

To identify the activity responsible for blocking association of mutant SOD1 with mitochondria, liver cytosol was incubated with proteinase K and the resultant peptides and other low molecular weight species below 10 KDa were removed by centrifugal filtration. Remaining proteins and other macromolecules were then fractionated by gel permeation chromatography (see schematic in Figure 2A). Finally, fractions were assayed for ability to inhibit recombinant $SOD1^{G85R}$ binding to non-transgenic mitochondria. Activity eluted broadly with apparent molecular weights between 12 and 45 kDa. Proteins in the fractions with activity (fractions 23-41, Figure 2C) were visualized by polyacrylamide gel electrophoresis and Coomassie staining (Figure 2B). The most slowly eluting fraction with activity (fraction 41) had only a handful of observable polypeptides (Figure 2B). We therefore used mass spectrometry to analyze its protein content. While the sensitivity of mass spectrometry frequently identifies many proteins present in such assays, remarkably however, only 7 proteins were detected (Figure 2D). One of these, profilin-1, an actin binding protein linked to regulation of actin polymerization, was notable as mutations in it are causative of a small proportion of inherited ALS (Wu et al., 2012). Nevertheless, immunoblotting was used to determine that profilin-1 was absent from many fractions (23-30) that retained inhibitory activity (Figure 2E).

Similar immunoblotting with antibodies to each of the six remaining proteins determined that only one co-fractionated with the inhibitory activity (Figure 2E). This was the 12 kDa macrophage migration inhibitory factor (MIF), which has previously been implicated in divergent functional roles: as a protein folding chaperone (Cherepkova et al., 2006), as a thiol-oxidoreductase protein (Kleemann et al., 1998), and as a secreted cytokine with an important role in innate immunity (Calandra and Roger, 2003; Lolis and Bucala, 2003). MIF eluted broadly in fractions spanning from 12 to 45 kDa apparent molecular weights, just as did the activity for inhibiting mutant SOD1 binding to mitochondria. The broad elution of MIF was not because of poor resolution of the column, as other proteins (including alcohol dehydrogenase, profilin-1 and SOD1 itself) fractionated much more sharply. Rather, the broad elution was fully consistent with MIF's known ability to form dimers and trimers (Mischke et al., 1998; Philo et al., 2004) through an exposed hydrophobic face as a part of its ATP-independent activity as a protein folding chaperone (Cherepkova et al., 2006). Interestingly, MIF protein levels do not change within the spinal cord during disease course in SOD1 mutant mice (Figure S2)

Dose dependent inhibition by MIF of mutant SOD1 association with mitochondria

As a direct test of whether MIF inhibits association of mutant SOD1 with mitochondria, purified mutant or wild type SOD1 (Figure 3A, bottom right) was added to normal liver mitochondria in the presence or absence of purified MIF (see schematic Figure 3A). After recovering the mitochondria by centrifugation, immunoblotting was used to reveal that a proportion of $SOD1^{G93A}$ and $SOD1^{G85R}$, but not $SOD1^{WT}$, bound to non-transgenic mitochondria in a dose dependent manner (Figure S3) in the absence of MIF (Figure 3B). Mutant SOD1 binding was inhibited in a dose dependent manner by co-incubation with MIF, with a 1:80 molar ratio of MIF to SOD1 (50 ng of MIF and 4 μg of mutant SOD1) sufficient to strongly diminish (by >90%) binding of mutant SOD1 to mitochondria (Figure

3C). Importantly, about 5 to 10% of recombinant mutant SOD1 bound to mitochondria in these assays (Figure 3C), a percentage of misfolded SOD1 similar to that measured in immunoprecipitates of the initial recombinant SOD1 preparation when using B8H10 antibodies that bind misfolded SOD1 (Figure S5).

We exploited the known proteinase K resistance or sensitivity, respectively, of correctly folded and misfolded $SOD1^{G93A}$ (Borchelt et al., 1994; Ratovitski et al., 1999) to test if the mutant SOD1 which associates with mitochondria represents the initially misfolded fraction. We initially verified that most of the dismutase active $SOD1^{G93A}$ is protease resistant; in contrast, most of the inactive $SOD1^{G85R}$ was sensitive (Figure 3E). $SOD1^{G93A}$ was pre-incubated with proteinase K, then the protease was inactivated by addition of PMSF and the mixture incubated with normal liver mitochondria, and finally mitochondria along with any bound mutant SOD1 recovered by centrifugation. Immunoblotting for human SOD1 demonstrated that $SOD1^{G93A}$ association with mitochondria was completely eliminated by proteinase K preincubation, confirming that the protease sensitive, misfolded fraction is the one that associates with mitochondria (Figure 3D).

Inhibition of misfolded SOD1 association with mitochondria was specific to MIF, as other chaperones tested, including Hsp27, Hsc70, aB-crystallin [previously reported to interact with mutant and misfolded SOD1 and modulate its aggregation (Karch and Borchelt, 2010; Krishnan et al., 2008; Wang et al., 2009; Wang et al., 2005; Yerbury et al., 2013; Zetterstrom et al., 2011b)], cyclophilin-A [one of our 7 candidate proteins and previously proposed to act as a chaperone (Freskgard et al., 1992)], or glutathione peroxidase [a protein with thiol-oxidoreductase activity, an activity that has been proposed to be crucial for the association of mutant SOD1 proteins with mitochondria (Cozzolino et al., 2008; Ferri et al., 2006)], had no effect on mutant SOD1 association with normal mitochondria (Figure 3F, G).

MIF suppresses misfolded mutant SOD1 association with ER and mitochondrial membranes in motor neuron-like cells

We next tested if MIF inhibited association of mutant SOD1 not only with mitochondria but also with other intracellular membranes in motor neuron-like (NSC-34) cells expressing ALS-linked SOD1 mutants (see schematic in Figure 4A). EGFP-tagged $SOD1^{G93A}$ or $SOD1^{G85R}$ were expressed by DNA transfection, along with lower or higher amounts of MIF. Accumulated levels were validated by immunoblotting for each protein (Figure 4B, bottom) and the association of mutant SOD1 with ER membranes was determined after isolation of microsomes. Both dismutase active ($SOD1^{G93A}$) and dismutase inactive ($SOD1^{G85R}$) mutants bound to ER membranes in the presence of the low endogenous levels of MIF – Figure 4B, lanes 1 and 4), but binding in both cases was reduced in a dose-dependent manner when MIF levels were elevated (Figure. 4B). MIF also inhibited mutant SOD1 association with mitochondria (Figure 4C).

We next tested if MIF also inhibited accumulation of misfolded SOD1 in a dose-dependent manner in the same motor neuron-like cells expressing ALS-linked SOD1 mutants (see schematic in Figure 4D). In the absence of transfected MIF, misfolded SOD1 accumulated and could be detected by immunoprecipitation with the B8H10 antibody which does not recognize wild type SOD1 but does recognize a wide spectrum of misfolded SOD1 mutants

(Gros-Louis et al., 2010) including SOD1^{G93A} and SOD1^{G85R} (Figure 4E, lanes 2 and 3). Transfection to simultaneously express MIF along with either SOD1^{G93A} or SOD1^{G85R} reduced the level of misfolded SOD1 (Figure 4E, lanes 4 and 5), without affecting the overall level of accumulated mutant SOD1. Similar results were observed by expressing MIF in the presence of untagged versions of SOD1^{G93A} or SOD1^{G85R} in human SH-SY5Y neuroblastoma cells (Figure S4).

The thiol-oxidoreductase activity of MIF is not necessary for suppressing misfolded SOD1

One of MIF's previously documented enzymatic roles is as a thiol-oxidoreductase (Kleemann et al., 1998). SOD1 monomers lacking the C57-C146 disulfide bond represent the major portion of misfolded SOD1 (Zetterstrom et al., 2013), thus suggesting that a thiol-oxidoreductase activity may play an important role in misfolded protein formation. To determine if the action of MIF in suppressing accumulation of misfolded SOD1 required this activity, cells were transfected with a point mutant of MIF (MIF^{C60S}) previously shown to completely lack oxidoreductase activity (Kleemann et al., 1998). Co-expression of MIF^{C60S} in NSC-34 cells with either SOD1^{G93A} or SOD1^{G85R} inhibited the accumulation of misfolded SOD1 in a dose-dependent manner (Figure 4F), consistent with an *in vivo* ability to suppress mutant SOD1 accumulation onto microsomal (Figure 4B) or mitochondrial membranes (Figure 4C). Misfolding of SOD1^{G93A}, which can acquire normal folding (as indicated by dimerization, protease resistance and high specific activity as a superoxide dismutase (Borchelt et al., 1994; Ratovitski et al., 1999)), was more effectively suppressed by MIF^{C60S} than was the dismutase inactive SOD1^{G85R} most of which cannot adopt a stable conformation that confers protease resistance (Figure 3E).

MIF directly suppresses the accumulation of misfolded SOD1 *in vitro*

To determine if MIF directly inhibits the accumulation of misfolded SOD1, immunoprecipitation was performed (see schematic in Figure 5A) with a previously reported conformation-specific antibody (DSE2) that selectively recognizes misfolded, but not correctly folded, SOD1 (Israelson et al., 2010; Vande Velde et al., 2008). As expected, a proportion of SOD1^{G93A} and SOD1^{G85R}, but not SOD1^{WT}, were immunoprecipitated with the DSE2 antibody (Figure 5B, lanes 3 and 5). Incubation of the mutant SOD1 with MIF nearly eliminated misfolded SOD1^{G93A} that could be immunoprecipitated by DSE2 (Figure 5B, lanes 3 versus 4). MIF also substantially inhibited accumulation of misfolded SOD1^{G85R} (Figure 5B, lanes 5 and 6). Remarkably, a similar level of inhibition was observed when the SOD1^{G85R} mutant was incubated with a liver cytosolic fraction that contained endogenous MIF accumulated to a similar level (Figure 5B, lane 7).

Next, purified SOD1^{G93A} was depleted of initially misfolded SOD1 by immunoprecipitation with the B8H10 antibody (Figure 5D, lane 2), the unbound fraction free of misfolded SOD1 was incubated at 37°C in the absence (lane 3) or presence (lane 4) of MIF, and finally newly generated misfolded SOD1 was detected with a second round of immunoprecipitation with B8H10 antibody. Remarkably, MIF suppressed formation of newly misfolded SOD1, as revealed by immunoblotting the final immunoprecipitate (Figure 5D, lane 4). Suppression was specific for MIF, since neither aB-crystallin nor Hsc70 (added at comparable concentrations) inhibited formation of newly misfolded SOD1 (Figure S6).

Possible direct binding of MIF to mutant SOD1 was tested by covalently labeling purified MIF with a green fluorescent dye (at a ratio of one labeled lysine residue per one MIF molecule) and incubating it with increasing concentrations of purified $SOD1^{G93A}$ (2.4 nM to 80 μM). Binding of the two was quantified using microscale thermophoresis (MST), a sensitive protein-protein interaction assay (Wienken et al., 2010) that measures changes in the thermal migration behavior of particles in a temperature gradient as influenced by a binding partner. By plotting the percentage of change in normalized fluorescence as a function of $SOD1^{G93A}$ concentration (Wienken et al., 2010), curve fitting to the data points produced an excellent fit with a calculated dissociation constant (K_d) of 367 nM for interaction of mutant $SOD1^{G93A}$ and MIF (Figure 5E).

A low level of endogenous MIF within motor neuron perikarya

Immunostaining for MIF in non-transgenic rat spinal cord revealed it to be accumulated widely with the striking exception of almost complete absence within ChAT-positive motor neuron cell bodies (Figure 6A). In contrast, MIF was readily detected in astrocytes (Figure 6B). While no change was apparent in overall MIF protein levels within the spinal cord during disease course (Figure S2), immunostaining revealed increased MIF in reactive astrocytes just after symptomatic onset (i.e., one week after the first fibrillation) in a $SOD1^{G93A}$ rat (Figure 6D and Figure S7). Nevertheless, MIF protein remained undetectable in motor neurons and this low level of intraperikaryal MIF was accompanied by accumulation of misfolded SOD1 (recognized by the B8H10 antibody) (Figure 6C, D; arrow in E and Figure S7).

To determine if the absence of accumulated MIF in motor neurons resulted from a low level (or absence) of synthesis of MIF in those neurons, we exploited bacTRAP reporter mouse lines (Doyle et al., 2008; Heiman et al., 2008) (see schematic in Figure 7A) that express an EGFP-tagged ribosomal protein L10a (Rpl10a) driven by cell type specific transgene promoters in motor neurons (*Chat*-bacTRAP), astrocytes (*Aldh1l1*-bacTRAP) or oligodendrocytes (*Cnp1*-bacTRAP) (Doyle et al., 2008; Heiman et al., 2008). Analysis of affinity isolated, actively translating, polyribosome-associated mRNAs from each cell type (Figure 7B) revealed that translating MIF mRNA was found in all three cell types, with motor neurons accumulating the highest level (Figure 7C). Thus, MIF is synthesized actively by motor neurons, and its low accumulation in motor neuron cell bodies (Figure 6) must be the result of rapid clearance (secretion, degradation or transport) from the perikarya of those neurons.

Increased MIF enhances survival of mutant SOD1-expressing motor neurons

To test if increased synthesis and accumulation of MIF could be protective of mutant SOD1-expressing motor neurons, motor neurons were isolated by fluorescent cell sorting for expression of an HB9-promoted GFP motor neuron reporter gene following differentiation from non-transgenic mouse embryonic stem cells or induced pluripotent stem (iPS) cells derived from mice expressing human wild type ($SOD1^{WT}$) or mutant ($SOD1^{G93A}$) SOD1 transgenes (see schematic in Figure 8A). MIF synthesis was elevated by transduction with a lentivirus encoding MIF and RFP (the latter translated from an internal ribosomal entry site (IRES) in the MIF 3′ untranslated region). Beginning day 3 post-transduction, intraneuronal

levels of MIF (detected by indirect immunofluorescence with MIF antibody) were elevated relative to motor neurons transduced with RFP alone (Figure 8B). The contrast between the failure of endogenously synthesized MIF to accumulate in mature motor neurons (Figure 6) and its accumulation via lentiviral transduction in cultured motor neurons (Figure 8) can be explained in two ways. Elevated MIF synthesis in cultured motor neurons may saturate degradation or secretion machineries. Alternatively, the degradation/secretion of endogenous MIF in mature motor neurons may reflect a non-cell autonomous influence, especially on secretion, exercised by the partner glial cells which are missing in our pure neuronal cultures.

Direct live-cell imaging (Figure 8C) revealed that, compared to non-transgenic or $SOD1^{WT}$ motor neurons, only $1/5^{th}$ as many mutant $SOD1^{G93A}$ expressing motor neurons survived the first two days of culture prior to MIF synthesis (Figure 8D-F). MIF expression, however, significantly attenuated this accelerated motor neuron death at subsequent time points (Figure 8F). Similarly, increased MIF significantly increased neurite length of the surviving $SOD1^{G93A}$ motor neurons (Figure 8G).

Discussion

Among the important unsolved questions in disease mechanism from ubiquitous expression of mutant SOD1 is what determines the selective, age-dependent motor neuronal degeneration that is accompanied by mutant SOD1 misfolding and its association with mitochondria and ER. We have now determined that both dismutase active and inactive SOD1 mutant association with such organelles can be suppressed by cytosolic MIF acting catalytically to inhibit misfolded SOD1 accumulation and its association with mitochondria and ER. Furthermore, increased MIF, which normally accumulates only to low levels within the cell bodies of motor neurons, suppresses misfolded SOD1 accumulation and extends mutant SOD1-expressing motor neuron survival in cell culture. The low level of MIF accumulated within motor neurons correlates with accumulation of misfolded SOD1 species and their association with different intracellular organelles within those neurons.

Despite its small size (12 kDa), MIF has previously been implicated in both extracellular and intracellular roles. MIF was one of the first cytokines to be described (George and Vaughan, 1962), with its action in the immune response upstream of tumor necrosis factor (TNF)-α, interleukin (IL)-1β, interferon (IFN)γ, and other effector cytokines (Calandra and Roger, 2003). MIF is synthesized as a cytoplasmic protein [a point we have validated after removal of even small vesicles from extracts of peripheral and nervous system tissues (Figure 2E)], with cytokine activity achieved by post-translational sequestration of cytoplasmic MIF into vesicles for release by an as yet unidentified mechanism in response to a variety of signals (Merk et al., 2009).

Intracellularly, MIF acts as a chaperone protein (Cherepkova et al., 2006) and a thiol-protein oxidoreductase (Kleemann et al., 1998). Its protein folding activity derives from switching from multimeric to monomeric forms, thereby exposing a hydrophobic surface that can provide ATP-independent chaperone activity. MIF's multiple activities parallel the well-known ATP-dependent protein chaperone Hsp70, for which dual roles as a chaperone and

cytokine have also been reported (Asea et al., 2000; Pockley et al., 2009). The ability of MIF to act as a thiol-protein oxidoreductase was initially of special interest to us for four primary reasons. First, a major portion of misfolded SOD1 has been proposed to be composed of SOD1 monomers lacking the C57-C146 disulfide bond (Zetterstrom et al., 2013). Second, mutant SOD1 proteins that associate with mitochondria have been reported to be partially oxidized (Ferri et al., 2006) and Cys-111 was reported to be necessary for mutant SOD1 association with mitochondria (Cozzolino et al., 2008; Ferri et al., 2006). Third, the thiol-reductase activity has been proposed to reduce oxidative stress and inhibit apoptosis (Nguyen et al., 2003). Finally, overexpression of glutaredoxin-1 or glutaredoxin-2, each with thiol-oxidoreductase activity, was reported to improve the solubility of the mutant SOD1 and to prevent its mitochondrial binding (Cozzolino et al., 2008; Ferri et al., 2010). Nevertheless, using a MIF mutant that lacks all thiol-oxidoreductase activity, we have demonstrated that it is chaperone, not thiol-oxidoreductase, activity of MIF that can inhibit mutant SOD1 misfolding and membrane association.

We would also note that nearly eliminating aggregated misfolded SOD1 (by increasing mitochondrial buffering of calcium by deletion of cyclophilin D) has no effect in ameliorating fatal disease progression in multiple SOD1 mutant mouse models (Parone et al., 2013). Hence, rather than highly aggregated forms as the toxic species, *in vivo* toxicity appears to derive from soluble, misfolded SOD1 which remained unaffected in the mice with reduced aggregated mutant SOD1. This is the SOD1 species that we have shown that MIF chaperone activity acts to reduce. Other chaperones previously linked to SOD1, including Hsp27, aB-crystallin and Hsc70, were unable to suppress mutant SOD1 binding to mitochondria or accumulation of newly formed misfolded SOD1. From these collective efforts, we now propose that low MIF chaperone-like activity in alpha motor neurons plays a pivotal role in misfolded SOD1 accumulation and subsequent toxicity.

Of relevance to MIF's extracellular activities, mutant SOD1 synthesized by microglia drives rapid disease progression (Beers et al., 2006; Boillee et al., 2006). Additionally, immunodeficiency shortened mutant SOD1 mouse life span (Beers et al., 2008; Chiu et al., 2008), while conversely, passive transfer of activated T regulatory cells to immunocompetent mice modestly extended survival (Beers et al., 2011). We note that one of the manifestations of immune deficits in ALS could be a malfunction of MIF, thereby leading to accumulation of soluble misfolded SOD1 and binding to intracellular targets. Indeed, recognizing the potential for cell-to-cell spread of misfolded SOD1 as a means of disease propagation (Grad and Cashman, 2014; Grad et al., 2011; Munch et al., 2011), chaperone activity by extracellular MIF may act to limit such spreading.

Finally, misfolded SOD1 has been reported by several groups to accumulate in motor neurons or glia in sporadic ALS (Bosco et al., 2010; Forsberg et al., 2011; Forsberg et al., 2010; Grad et al., 2014; Guareschi et al., 2012; Kabashi et al., 2007; Pokrishevsky et al., 2012; Zetterstrom et al., 2011a), although other efforts have reached opposite conclusions (Ayers et al., 2014; Brotherton et al., 2012; Kerman et al., 2010; Liu et al., 2009). Astrocytes generated from neural precursor cells (NPCs) isolated from spinal cords of sporadic ALS patients have been found to be toxic to co-cultured motor neurons (Haidet-Phillips et al., 2011), similar to what had been seen previously for astrocytes expressing mutant SOD1 (Di

Giorgio et al., 2007; Marchetto et al., 2008; Nagai et al., 2007). Surprisingly, reducing wild-type SOD1 with shRNA significantly reduced toxicity to motor neurons of most of the "sporadic" ALS astrocytes (Haidet-Phillips et al., 2011), a finding directly disputed by others who concluded that wild type SOD1 plays no role in the toxicity of sporadic ALS-derived astrocytes to co-cultured motor neurons (Re et al., 2014).

The controversy notwithstanding, misfolded protein accumulation is central to essentially all instances of inherited and sporadic ALS. Identification of MIF as an intracellular chaperone that stimulates folding/refolding of misfolded SOD1 suggests a new avenue for therapy development in ALS through increasing intracellular MIF levels. Combined with recognition that extracellular MIF is an inducer of metalloproteinase 9 (MMP9) (Yu et al., 2007), a component contributing to the selectivity of motor neuron vulnerability to SOD1 mutant-mediated death (Kaplan et al., 2014), this finding underscores how approaches to increase intracellular MIF (e.g., by reducing its clearance from motor neurons) and/or to inhibit its induction of MMP9 (e.g., with drugs that block MIF's interaction with its known receptor (CD74) (Bai et al., 2012)) could be attractive therapeutic strategies.

Experimental Procedures

Transgenic animals

Transgenic rats expressing hSOD1^{WT} (Chan et al., 1998), hSOD1^{G93A} (Howland et al., 2002) and hSOD1^{H46R} (Nagai et al., 2001) were as originally described. Transgenic mice expressing mutant SOD1^{G85R} (line 148), SOD1^{G37R} (line 42), or SOD1^{G93A} were maintained by standard protocols in the Cleveland laboratory. bacTRAP transgenic mouse lines: *Chat-bacTRAP* line expresses an EGFP-tagged ribosome protein Rpl10a only within motor neurons. The *Aldh1l1*-bacTRAP line expresses the same EGFP-tagged Rpl10a in astrocytes, while the *Cnp1*-bacTRAP expresses in mature oligodendrocytes (Doyle et al., 2008; Heiman et al., 2008). All animal procedures were consistent with the requirements of the Animal Care and Use Committee of the University of California.

Mutant SOD1 binding to mitochondria

Spinal cord or liver cytosolic fractions (200 μg) from hSOD1^{G93A} (∼90 d old) or hSOD1^{H46R} (∼ 200 d old) symptomatic female rats or recombinant hSOD1^{WT}, hSOD1^{G93A} or hSOD1^{G85R} proteins (4 μg) were incubated with spinal cord or liver mitochondria (50 μg) isolated from non-transgenic rats for 30 min at 37°C in the presence or absence of recombinant mouse MIF (R&D Systems) at the indicated concentration. Where indicated, the recombinant mutant SOD1 was incubated with Proteinase K (100 μg/ml) for 15 min. The reaction was stopped by addition of 10 mM PMSF followed by incubation on ice for 10 min. Then, the mitochondrial fraction was recovered by centrifugation at 12,000 × g for 10 min at 4°C and washed twice with mitochondrial buffer. The pellet was resuspended with sample buffer and run by SDS-PAGE.

iPSC cell generation

Neuronal progenitor cells (NPCs), expressing the motor neuron Hb9: :GFP reporter, obtained from SOD1^{WT} and SOD1^{G93A} mice were converted to iPSCs. As previously

described, retrovirus encoding OCT3/4 and KLF4 were sufficient to generate iPSC clones (Hester et al., 2009; Kim et al., 2008). Twenty viral particles per cell were needed to efficiently reprogram the cells. Cells were cultured in the presence of NPC media for four days followed by a change to mouse embryonic stem cell (mESC) media with DMEM (Millipore, Billerica, MA), supplemented with 18% ES FBS (Invitrogen), L-glutamine (2mM, Invitrogen), nonessential amino acids (1×, Millipore), antibiotic-antimycotic (Invitrogen), 2-mercaptoethanol (Sigma), and recombinant LIF (100U/ml, Millipore). iPSC clones were morphologically similar to mouse ESCs (HBG3 cells, Thomas Jessell, Columbia University) and were obtained within two weeks. A wide panel of markers was used to compare ESCs with the newly generated iPSC lines and found no significant difference for their expression between cell lines.

Mouse motor neuron differentiation

Mouse ESCs or iPSCs expressing Hb9: :GFP reporter were cultured on top of inactivated mouse fibroblasts (Millipore). Motor neuron differentiation was induced by plating 1-2 × 10^6 mES cells per 10 cm dish in the presence of 2 μM retinoic acid (Sigma-Aldrich) and 2 μM purmorphamine (Calbiochem, Billerica, MA). After 5 days of differentiation, embryonic bodies were dissociated and sorted based on levels of GFP using a FACSVantage/DiVa sorter (BD Biosciences, Rockville, MD).

Expression of MIF in mouse motor neurons and analysis

To express MIF in motor neurons, a previously described protocol was followed, with minor modifications (Kaech and Banker, 2006). Briefly, sorted GFP+ motor neurons were plated at a density of 15,000 cells per well on a laminin-coated 96 well plate. 12 hours after plating, the cells were infected with lentivirus to overexpress transgenes (40 viral particles per MN). Motor neuron cultures were allowed to continue for another 5 days, with half of the media being replaced every other day. RFP could be detected after 72 hours post-infection. At various time points during the culture of motor neurons, images were recorded using a fully automated IN CELL 6000 cell imager (GE Healthcare) as previously reported (Meyer et al., 2014). Images were further processed with the Developer and Analyzer software package (GE Healthcare) for survival counts and neurite length measurements. Otherwise noted, images shown represent 120 hours post infection. All counts were performed in triplicate and repeated at least three times.

Supplementary Material

Refer to Web version on PubMed Central for supplementary material.

Acknowledgments

We would like to thank Jean-Pierre Julien for the pEGFP-SOD1 vectors, Jurgen Bernhagen for providing the MIF vectors and Neil Cashman for the DSE2 antibodies. We thank Alex Kopelevich, Jon Artates and Amanda Seelman for their technical assistance and Jennifer Santini for technical support at the UCSD Microscopy Core Facility, supported by UCSD Neuroscience Microscopy Shared Facility Grant P30 NS047101. This work has been supported by grants from the NIH (R01 NS27036 to D.W.C. and R01 NS644912 to B.K.K). A.I. has been supported by a career development grant from the Muscular Dystrophy Association (MDA) and a Marie Curie Career Integration Grant (CIG). D.D. is supported by an NIH postdoctoral fellowship. D.W.C. receives salary support from the Ludwig Institute for Cancer Research.

Literature Cited

Asea A, Kraeft SK, Kurt-Jones EA, Stevenson MA, Chen LB, Finberg RW, Koo GC, Calderwood SK. HSP70 stimulates cytokine production through a CD14-dependant pathway, demonstrating its dual role as a chaperone and cytokine. Nature medicine. 2000; 6:435–442.

Ayers JI, Xu G, Pletnikova O, Troncoso JC, Hart PJ, Borchelt DR. Conformational specificity of the C4F6 SOD1 antibody; low frequency of reactivity in sporadic ALS cases. Acta neuropathologica communications. 2014; 2:55. [PubMed: 24887207]

Bai F, Asojo OA, Cirillo P, Ciustea M, Ledizet M, Aristoff PA, Leng L, Koski RA, Powell TJ, Bucala R, et al. A novel allosteric inhibitor of macrophage migration inhibitory factor (MIF). The Journal of biological chemistry. 2012; 287:30653–30663. [PubMed: 22782901]

Beers DR, Henkel JS, Xiao Q, Zhao W, Wang J, Yen AA, Siklos L, McKercher SR, Appel SH. Wild-type microglia extend survival in PU.1 knockout mice with familial amyotrophic lateral sclerosis. Proc Natl Acad Sci U S A. 2006; 103:16021–16026. [PubMed: 17043238]

Beers DR, Henkel JS, Zhao W, Wang J, Appel SH. CD4+ T cells support glial neuroprotection, slow disease progression, and modify glial morphology in an animal model of inherited ALS. Proc Natl Acad Sci U S A. 2008; 105:15558–15563. [PubMed: 18809917]

Beers DR, Henkel JS, Zhao W, Wang J, Huang A, Wen S, Liao B, Appel SH. Endogenous regulatory T lymphocytes ameliorate amyotrophic lateral sclerosis in mice and correlate with disease progression in patients with amyotrophic lateral sclerosis. Brain. 2011; 134:1293–1314. [PubMed: 21596768]

Boillee S, Yamanaka K, Lobsiger CS, Copeland NG, Jenkins NA, Kassiotis G, Kollias G, Cleveland DW. Onset and progression in inherited ALS determined by motor neurons and microglia. Science. 2006; 312:1389–1392. [PubMed: 16741123]

Borchelt DR, Lee MK, Slunt HS, Guarnieri M, Xu ZS, Wong PC, Brown RH Jr, Price DL, Sisodia SS, Cleveland DW. Superoxide dismutase 1 with mutations linked to familial amyotrophic lateral sclerosis possesses significant activity. Proc Natl Acad Sci U S A. 1994; 91:8292–8296. [PubMed: 8058797]

Bosco DA, Morfini G, Karabacak NM, Song Y, Gros-Louis F, Pasinelli P, Goolsby H, Fontaine BA, Lemay N, McKenna-Yasek D, et al. Wild-type and mutant SOD1 share an aberrant conformation and a common pathogenic pathway in ALS. Nat Neurosci. 2010; 13:1396–1403. [PubMed: 20953194]

Brotherton TE, Li Y, Cooper D, Gearing M, Julien JP, Rothstein JD, Boylan K, Glass JD. Localization of a toxic form of superoxide dismutase 1 protein to pathologically affected tissues in familial ALS. Proceedings of the National Academy of Sciences of the United States of America. 2012; 109:5505–5510. [PubMed: 22431618]

Calandra T, Roger T. Macrophage migration inhibitory factor: a regulator of innate immunity. Nature reviews Immunology. 2003; 3:791–800.

Chan PH, Kawase M, Murakami K, Chen SF, Li Y, Calagui B, Reola L, Carlson E, Epstein CJ. Overexpression of SOD1 in transgenic rats protects vulnerable neurons against ischemic damage after global cerebral ischemia and reperfusion. J Neurosci. 1998; 18:8292–8299. [PubMed: 9763473]

Cherepkova OA, Lyutova EM, Eronina TB, Gurvits BY. Chaperone-like activity of macrophage migration inhibitory factor. Int J Biochem Cell Biol. 2006; 38:43–55. [PubMed: 16099194]

Chiu IM, Chen A, Zheng Y, Kosaras B, Tsiftsoglou SA, Vartanian TK, Brown RH Jr, Carroll MC. T lymphocytes potentiate endogenous neuroprotective inflammation in a mouse model of ALS. Proc Natl Acad Sci U S A. 2008; 105:17913–17918. [PubMed: 18997009]

Cozzolino M, Amori I, Pesaresi MG, Ferri A, Nencini M, Carri MT. Cysteine 111 affects aggregation and cytotoxicity of mutant Cu,Zn-superoxide dismutase associated with familial amyotrophic lateral sclerosis. J Biol Chem. 2008; 283:866–874. [PubMed: 18006498]

Da Cruz S, Cleveland DW. Understanding the role of TDP-43 and FUS/TLS in ALS and beyond. Current opinion in neurobiology. 2011; 21:904–919. [PubMed: 21813273]

Di Giorgio FP, Carrasco MA, Siao MC, Maniatis T, Eggan K. Non-cell autonomous effect of glia on motor neurons in an embryonic stem cell-based ALS model. Nat Neurosci. 2007; 10:608–614. [PubMed: 17435754]

Doyle JP, Dougherty JD, Heiman M, Schmidt EF, Stevens TR, Ma G, Bupp S, Shrestha P, Shah RD, Doughty ML, et al. Application of a translational profiling approach for the comparative analysis of CNS cell types. Cell. 2008; 135:749–762. [PubMed: 19013282]

Ferri A, Cozzolino M, Crosio C, Nencini M, Casciati A, Gralla EB, Rotilio G, Valentine JS, Carri MT. Familial ALS-superoxide dismutases associate with mitochondria and shift their redox potentials. Proc Natl Acad Sci U S A. 2006; 103:13860–13865. [PubMed: 16945901]

Ferri A, Fiorenzo P, Nencini M, Cozzolino M, Pesaresi MG, Valle C, Sepe S, Moreno S, Carri MT. Glutaredoxin 2 prevents aggregation of mutant SOD1 in mitochondria and abolishes its toxicity. Human molecular genetics. 2010; 19:4529–4542. [PubMed: 20829229]

Forsberg K, Andersen PM, Marklund SL, Brannstrom T. Glial nuclear aggregates of superoxide dismutase-1 are regularly present in patients with amyotrophic lateral sclerosis. Acta Neuropathol. 2011; 121:623–634. [PubMed: 21287393]

Forsberg K, Jonsson PA, Andersen PM, Bergemalm D, Graffmo KS, Hultdin M, Jacobsson J, Rosquist R, Marklund SL, Brannstrom T. Novel antibodies reveal inclusions containing non-native SOD1 in sporadic ALS patients. PloS one. 2010; 5:e11552. [PubMed: 20644736]

Freskgard PO, Bergenhem N, Jonsson BH, Svensson M, Carlsson U. Isomerase and chaperone activity of prolyl isomerase in the folding of carbonic anhydrase. Science. 1992; 258:466–468. [PubMed: 1357751]

Fujisawa T, Homma K, Yamaguchi N, Kadowaki H, Tsuburaya N, Naguro I, Matsuzawa A, Takeda K, Takahashi Y, Goto J, et al. A novel monoclonal antibody reveals a conformational alteration shared by amyotrophic lateral sclerosis-linked SOD1 mutants. Ann Neurol. 2012; 72:739–749. [PubMed: 23280792]

George M, Vaughan JH. In vitro cell migration as a model for delayed hypersensitivity. Proc Soc Exp Biol Med. 1962; 111:514–521. [PubMed: 13947220]

Grad LI, Cashman NR. Prion-like activity of Cu/Zn superoxide dismutase: Implications for amyotrophic lateral sclerosis. Prion. 2014; 8

Grad LI, Guest WC, Yanai A, Pokrishevsky E, O'Neill MA, Gibbs E, Semenchenko V, Yousefi M, Wishart DS, Plotkin SS, et al. Intermolecular transmission of superoxide dismutase 1 misfolding in living cells. Proceedings of the National Academy of Sciences of the United States of America. 2011; 108:16398–16403. [PubMed: 21930926]

Grad LI, Yerbury JJ, Turner BJ, Guest WC, Pokrishevsky E, O'Neill MA, Yanai A, Silverman JM, Zeineddine R, Corcoran L, et al. Intercellular propagated misfolding of wild-type Cu/Zn superoxide dismutase occurs via exosome-dependent and -independent mechanisms. Proceedings of the National Academy of Sciences of the United States of America. 2014; 111:3620–3625. [PubMed: 24550511]

Gros-Louis F, Soucy G, Lariviere R, Julien JP. Intracerebroventricular infusion of monoclonal antibody or its derived Fab fragment against misfolded forms of SOD1 mutant delays mortality in a mouse model of ALS. J Neurochem. 2010; 113:1188–1199. [PubMed: 20345765]

Guareschi S, Cova E, Cereda C, Ceroni M, Donetti E, Bosco DA, Trotti D, Pasinelli P. An over-oxidized form of superoxide dismutase found in sporadic amyotrophic lateral sclerosis with bulbar onset shares a toxic mechanism with mutant SOD1. Proceedings of the National Academy of Sciences of the United States of America. 2012; 109:5074–5079. [PubMed: 22416121]

Haidet-Phillips AM, Hester ME, Miranda CJ, Meyer K, Braun L, Frakes A, Song S, Likhite S, Murtha MJ, Foust KD, et al. Astrocytes from familial and sporadic ALS patients are toxic to motor neurons. Nature biotechnology. 2011; 29:824–828.

Heiman M, Schaefer A, Gong S, Peterson JD, Day M, Ramsey KE, Suarez-Farinas M, Schwarz C, Stephan DA, Surmeier DJ, et al. A translational profiling approach for the molecular characterization of CNS cell types. Cell. 2008; 135:738–748. [PubMed: 19013281]

Hester ME, Song S, Miranda CJ, Eagle A, Schwartz PH, Kaspar BK. Two factor reprogramming of human neural stem cells into pluripotency. PloS one. 2009; 4:e7044. [PubMed: 19763260]

Howland DS, Liu J, She Y, Goad B, Maragakis NJ, Kim B, Erickson J, Kulik J, DeVito L, Psaltis G, et al. Focal loss of the glutamate transporter EAAT2 in a transgenic rat model of SOD1 mutant-mediated amyotrophic lateral sclerosis (ALS). Proc Natl Acad Sci U S A. 2002; 99:1604–1609. [PubMed: 11818550]

Ilieva H, Polymenidou M, Cleveland DW. Non-cell autonomous toxicity in neurodegenerative disorders: ALS and beyond. J Cell Biol. 2009; 187:761–772. [PubMed: 19951898]

Israelson A, Arbel N, Da Cruz S, Ilieva H, Yamanaka K, Shoshan-Barmatz V, Cleveland DW. Misfolded mutant SOD1 directly inhibits VDAC1 conductance in a mouse model of inherited ALS. Neuron. 2010; 67:575–587. [PubMed: 20797535]

Jerabek-Willemsen M, Wienken CJ, Braun D, Baaske P, Duhr S. Molecular interaction studies using microscale thermophoresis. Assay and drug development technologies. 2011; 9:342–353. [PubMed: 21812660]

Kabashi E, Valdmanis PN, Dion P, Rouleau GA. Oxidized/misfolded superoxide dismutase-1: the cause of all amyotrophic lateral sclerosis? Ann Neurol. 2007; 62:553–559. [PubMed: 18074357]

Kaech S, Banker G. Culturing hippocampal neurons. Nature protocols. 2006; 1:2406–2415.

Kaplan A, Spiller KJ, Towne C, Kanning KC, Choe GT, Geber A, Akay T, Aebischer P, Henderson CE. Neuronal matrix metalloproteinase-9 is a determinant of selective neurodegeneration. Neuron. 2014; 81:333–348. [PubMed: 24462097]

Karch CM, Borchelt DR. An examination of alpha B-crystallin as a modifier of SOD1 aggregate pathology and toxicity in models of familial amyotrophic lateral sclerosis. Journal of neurochemistry. 2010; 113:1092–1100. [PubMed: 20067574]

Kerman A, Liu HN, Croul S, Bilbao J, Rogaeva E, Zinman L, Robertson J, Chakrabartty A. Amyotrophic lateral sclerosis is a non-amyloid disease in which extensive misfolding of SOD1 is unique to the familial form. Acta Neuropathol. 2010; 119:335–344. [PubMed: 20111867]

Kim JB, Zaehres H, Wu G, Gentile L, Ko K, Sebastiano V, Arauzo-Bravo MJ, Ruau D, Han DW, Zenke M, et al. Pluripotent stem cells induced from adult neural stem cells by reprogramming with two factors. Nature. 2008; 454:646–650. [PubMed: 18594515]

Kleemann R, Kapurniotu A, Frank RW, Gessner A, Mischke R, Flieger O, Juttner S, Brunner H, Bernhagen J. Disulfide analysis reveals a role for macrophage migration inhibitory factor (MIF) as thiol-protein oxidoreductase. Journal of molecular biology. 1998; 280:85–102. [PubMed: 9653033]

Krishnan J, Vannuvel K, Andries M, Waelkens E, Robberecht W, Van Den Bosch L. Over-expression of Hsp27 does not influence disease in the mutant SOD1(G93A) mouse model of amyotrophic lateral sclerosis. Journal of neurochemistry. 2008; 106:2170–2183. [PubMed: 18624915]

Li Q, Vande Velde C, Israelson A, Xie J, Bailey AO, Dong MQ, Chun SJ, Roy T, Winer L, Yates JR, et al. ALS-linked mutant superoxide dismutase 1 (SOD1) alters mitochondrial protein composition and decreases protein import. Proc Natl Acad Sci U S A. 2010; 107:21146–21151. [PubMed: 21078990]

Liu HN, Sanelli T, Horne P, Pioro EP, Strong MJ, Rogaeva E, Bilbao J, Zinman L, Robertson J. Lack of evidence of monomer/misfolded superoxide dismutase-1 in sporadic amyotrophic lateral sclerosis. Ann Neurol. 2009; 66:75–80. [PubMed: 19670443]

Liu J, Lillo C, Jonsson PA, Vande Velde C, Ward CM, Miller TM, Subramaniam JR, Rothstein JD, Marklund S, Andersen PM, et al. Toxicity of familial ALS-linked SOD1 mutants from selective recruitment to spinal mitochondria. Neuron. 2004; 43:5–17. [PubMed: 15233913]

Lolis E, Bucala R. Macrophage migration inhibitory factor. Expert opinion on therapeutic targets. 2003; 7:153–164. [PubMed: 12667094]

Marchetto MC, Muotri AR, Mu Y, Smith AM, Cezar GG, Gage FH. Non-cell-autonomous effect of human SOD1 G37R astrocytes on motor neurons derived from human embryonic stem cells. Cell Stem Cell. 2008; 3:649–657. [PubMed: 19041781]

Mattiazzi M, D'Aurelio M, Gajewski CD, Martushova K, Kiaei M, Beal MF, Manfredi G. Mutated human SOD1 causes dysfunction of oxidative phosphorylation in mitochondria of transgenic mice. The Journal of biological chemistry. 2002; 277:29626–29633. [PubMed: 12050154]

Merk M, Baugh J, Zierow S, Leng L, Pal U, Lee SJ, Ebert AD, Mizue Y, Trent JO, Mitchell R, et al. The Golgi-associated protein p115 mediates the secretion of macrophage migration inhibitory factor. J Immunol. 2009; 182:6896–6906. [PubMed: 19454686]

Meyer K, Ferraiuolo L, Miranda CJ, Likhite S, McElroy S, Renusch S, Ditsworth D, Lagier-Tourenne C, Smith RA, Ravits J, et al. Direct conversion of patient fibroblasts demonstrates non-cell autonomous toxicity of astrocytes to motor neurons in familial and sporadic ALS. Proceedings of the National Academy of Sciences of the United States of America. 2014; 111:829–832. [PubMed: 24379375]

Mischke R, Kleemann R, Brunner H, Bernhagen J. Cross-linking and mutational analysis of the oligomerization state of the cytokine macrophage migration inhibitory factor (MIF). FEBS letters. 1998; 427:85–90. [PubMed: 9613605]

Munch C, O'Brien J, Bertolotti A. Prion-like propagation of mutant superoxide dismutase-1 misfolding in neuronal cells. Proceedings of the National Academy of Sciences of the United States of America. 2011; 108:3548–3553. [PubMed: 21321227]

Nagai M, Aoki M, Miyoshi I, Kato M, Pasinelli P, Kasai N, Brown RH Jr, Itoyama Y. Rats expressing human cytosolic copper-zinc superoxide dismutase transgenes with amyotrophic lateral sclerosis: associated mutations develop motor neuron disease. J Neurosci. 2001; 21:9246–9254. [PubMed: 11717358]

Nagai M, Re DB, Nagata T, Chalazonitis A, Jessell TM, Wichterle H, Przedborski S. Astrocytes expressing ALS-linked mutated SOD1 release factors selectively toxic to motor neurons. Nat Neurosci. 2007; 10:615–622. [PubMed: 17435755]

Nguyen MT, Lue H, Kleemann R, Thiele M, Tolle G, Finkelmeier D, Wagner E, Braun A, Bernhagen J. The cytokine macrophage migration inhibitory factor reduces pro-oxidative stress-induced apoptosis. Journal of immunology. 2003; 170:3337–3347.

Nishitoh H, Kadowaki H, Nagai A, Maruyama T, Yokota T, Fukutomi H, Noguchi T, Matsuzawa A, Takeda K, Ichijo H. ALS-linked mutant SOD1 induces ER stress- and ASK1-dependent motor neuron death by targeting Derlin-1. Genes Dev. 2008; 22:1451–1464. [PubMed: 18519638]

Parker JL, Newstead S. Molecular basis of nitrate uptake by the plant nitrate transporter NRT1.1. Nature. 2014; 507:68–72. [PubMed: 24572366]

Parone PA, Da Cruz S, Han JS, McAlonis-Downes M, Vetto AP, Lee SK, Tseng E, Cleveland DW. Enhancing mitochondrial calcium buffering capacity reduces aggregation of misfolded SOD1 and motor neuron cell death without extending survival in mouse models of inherited amyotrophic lateral sclerosis. The Journal of neuroscience: the official journal of the Society for Neuroscience. 2013; 33:4657–4671. [PubMed: 23486940]

Pedrini S, Sau D, Guareschi S, Bogush M, Brown RH Jr, Naniche N, Kia A, Trotti D, Pasinelli P. ALS-linked mutant SOD1 damages mitochondria by promoting conformational changes in Bcl-2. Human molecular genetics. 2010

Philo JS, Yang TH, LaBarre M. Re-examining the oligomerization state of macrophage migration inhibitory factor (MIF) in solution. Biophysical chemistry. 2004; 108:77–87. [PubMed: 15043922]

Pockley AG, Calderwood SK, Multhoff G. The atheroprotective properties of Hsp70: a role for Hsp70-endothelial interactions? Cell Stress Chaperones. 2009; 14:545–553. [PubMed: 19357992]

Pokrishevsky E, Grad LI, Yousefi M, Wang J, Mackenzie IR, Cashman NR. Aberrant localization of FUS and TDP43 is associated with misfolding of SOD1 in amyotrophic lateral sclerosis. PLoS One. 2012; 7:e35050. [PubMed: 22493728]

Ratovitski T, Corson LB, Strain J, Wong P, Cleveland DW, Culotta VC, Borchelt DR. Variation in the biochemical/biophysical properties of mutant superoxide dismutase 1 enzymes and the rate of disease progression in familial amyotrophic lateral sclerosis kindreds. Human molecular genetics. 1999; 8:1451–1460. [PubMed: 10400992]

Re DB, Le Verche V, Yu C, Amoroso MW, Politi KA, Phani S, Ikiz B, Hoffmann L, Koolen M, Nagata T, et al. Necroptosis Drives Motor Neuron Death in Models of Both Sporadic and Familial ALS. Neuron. 2014

Rosen DR, Siddique T, Patterson D, Figlewicz DA, Sapp P, Hentati A, Donaldson D, Goto J, O'Regan JP, Deng HX, et al. Mutations in Cu/Zn superoxide dismutase gene are associated with familial amyotrophic lateral sclerosis. Nature. 1993; 362:59–62. [PubMed: 8446170]

Vande Velde C, McDonald KK, Boukhedimi Y, McAlonis-Downes M, Lobsiger CS, Bel Hadj S, Zandona A, Julien JP, Shah SB, Cleveland DW. Misfolded SOD1 associated with motor neuron mitochondria alters mitochondrial shape and distribution prior to clinical onset. PLoS One. 2011; 6:e22031. [PubMed: 21779368]

Vande Velde C, Miller TM, Cashman NR, Cleveland DW. Selective association of misfolded ALS-linked mutant SOD1 with the cytoplasmic face of mitochondria. Proc Natl Acad Sci U S A. 2008; 105:4022–4027. [PubMed: 18296640]

Wang J, Farr GW, Zeiss CJ, Rodriguez-Gil DJ, Wilson JH, Furtak K, Rutkowski DT, Kaufman RJ, Ruse CI, Yates JR 3rd, et al. Progressive aggregation despite chaperone associations of a mutant SOD1-YFP in transgenic mice that develop ALS. Proceedings of the National Academy of Sciences of the United States of America. 2009; 106:1392–1397. [PubMed: 19171884]

Wang J, Xu G, Li H, Gonzales V, Fromholt D, Karch C, Copeland NG, Jenkins NA, Borchelt DR. Somatodendritic accumulation of misfolded SOD1-L126Z in motor neurons mediates degeneration: alphaB-crystallin modulates aggregation. Human molecular genetics. 2005; 14:2335–2347. [PubMed: 16000321]

Wienken CJ, Baaske P, Rothbauer U, Braun D, Duhr S. Protein-binding assays in biological liquids using microscale thermophoresis. Nature communications. 2010; 1:100.

Wu CH, Fallini C, Ticozzi N, Keagle PJ, Sapp PC, Piotrowska K, Lowe P, Koppers M, McKenna-Yasek D, Baron DM, et al. Mutations in the profilin 1 gene cause familial amyotrophic lateral sclerosis. Nature. 2012; 488:499–503. [PubMed: 22801503]

Yerbury JJ, Gower D, Vanags L, Roberts K, Lee JA, Ecroyd H. The small heat shock proteins alphaB-crystallin and Hsp27 suppress SOD1 aggregation in vitro. Cell stress & chaperones. 2013; 18:251–257. [PubMed: 22993064]

Yu X, Lin SG, Huang XR, Bacher M, Leng L, Bucala R, Lan HY. Macrophage migration inhibitory factor induces MMP-9 expression in macrophages via the MEK-ERK MAP kinase pathway. Journal of interferon & cytokine research: the official journal of the International Society for Interferon and Cytokine Research. 2007; 27:103–109.

Zetterstrom P, Andersen PM, Brannstrom T, Marklund SL. Misfolded superoxide dismutase-1 in CSF from amyotrophic lateral sclerosis patients. Journal of neurochemistry. 2011a; 117:91–99. [PubMed: 21226712]

Zetterstrom P, Graffmo KS, Andersen PM, Brannstrom T, Marklund SL. Proteins that bind to misfolded mutant superoxide dismutase-1 in spinal cords from transgenic amyotrophic lateral sclerosis (ALS) model mice. The Journal of biological chemistry. 2011b; 286:20130–20136. [PubMed: 21493711]

Zetterstrom P, Graffmo KS, Andersen PM, Brannstrom T, Marklund SL. Composition of soluble misfolded superoxide dismutase-1 in murine models of amyotrophic lateral sclerosis. Neuromolecular medicine. 2013; 15:147–158. [PubMed: 23076707]

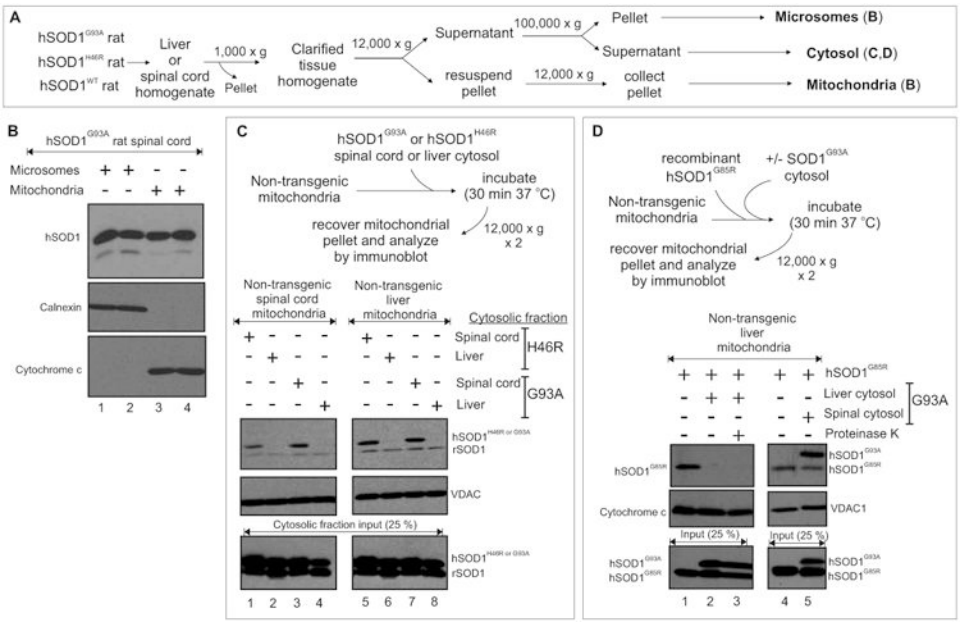

Figure 1. The cytosol determines mutant SOD1 association with mitochondria

(**A**) Schematic outlining purification steps for isolation of microsomes, cytosol and mitochondria from liver or spinal cord. (**B**) Immunoblot assay for mutant SOD1 associated with microsomes or mitochondria purified as in (**A**) from SOD1^{G93A} rat spinal cord. Calnexin and cytochrome c immunoblots were used as specific markers for microsomal and mitochondrial fractions, respectively. (**C**) Cytosol from SOD1^{G93A} or SOD1^{H46R} expressing rats were incubated with non-transgenic spinal cord or liver derived mitochondria and the mitochondria were recovered and analyzed by immunoblotting for bound mutant SOD1. Immunoblotting for VDAC1 was used to verify numbers of mitochondria recovered from each assay. (Bottom) Input cytosols were immunoblotted to identify the initial levels of human mutant SOD1 and endogenous rat SOD1. (**D**) Recombinant mutant SOD1^{G85R} was incubated with non-transgenic liver mitochondria in the absence or presence of liver or spinal cord cytosol from SOD1^{G93A} rats. Mitochondria were recovered and assayed by immunoblotting for whether addition of spinal cord or liver cytosol affected recruitment of SOD1^{G85R} to mitochondria. Mitochondrial recovery was assessed by immmunoblotting for VDAC1 or cytochrome c. The two lanes from the right panel were not loaded in the same order as shown.

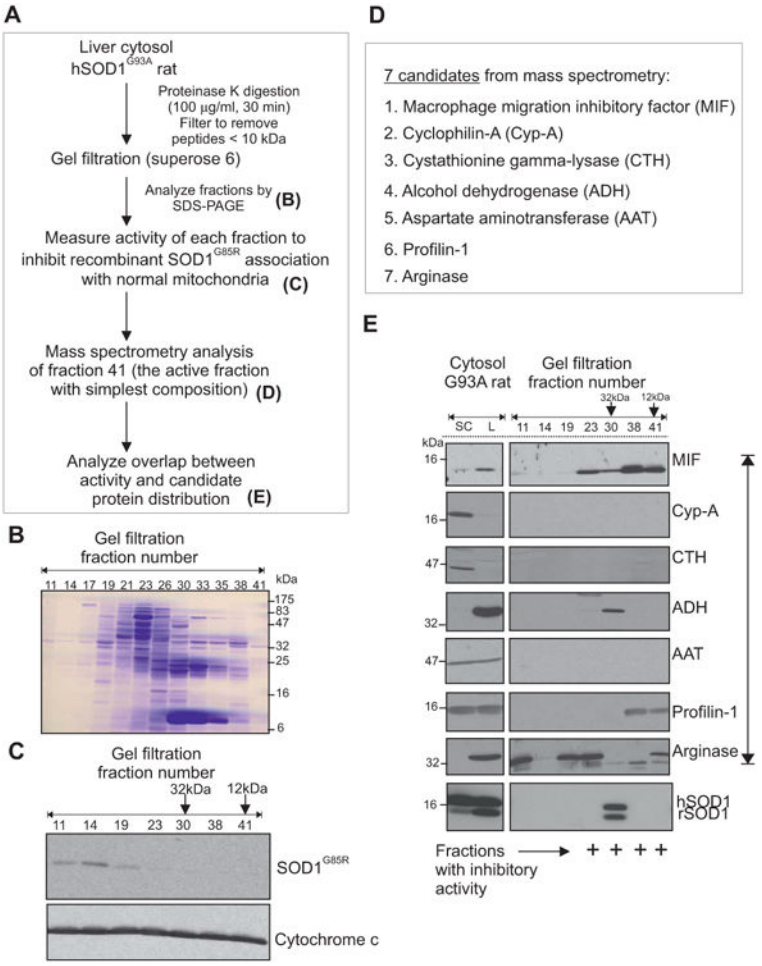

Figure 2. Identification of MIF as an activity that can suppress mutant SOD1 association with mitochondria

(**A**) Schematic outlining the purification steps of an activity in liver cytosol that inhibits mutant SOD1 association with normal mitochondria, followed by mass spectrometry to identify remaining proteins. (**B**) Coomassie staining of an SDS-polyacrylamide gel of gel filtration fractions from (**A**). (**C**) Assay of gel filtration fractions from (**A, B**) for presence of an activity that inhibits association of recombinant mutant SOD1^{G85R} with normal liver mitochondria. (**D**) The seven proteins identified by mass spectrometry to be present within gel filtration fraction 41 from (**C**), which contained activity inhibiting recombinant SOD1 binding to non-transgenic liver mitochondria and had the simplest protein composition. (**E**) Immunoblotting of gel filtration fractions for presence of each of the seven candidate proteins identified in (**D**). Only MIF co-fractionated with inhibitory activity.

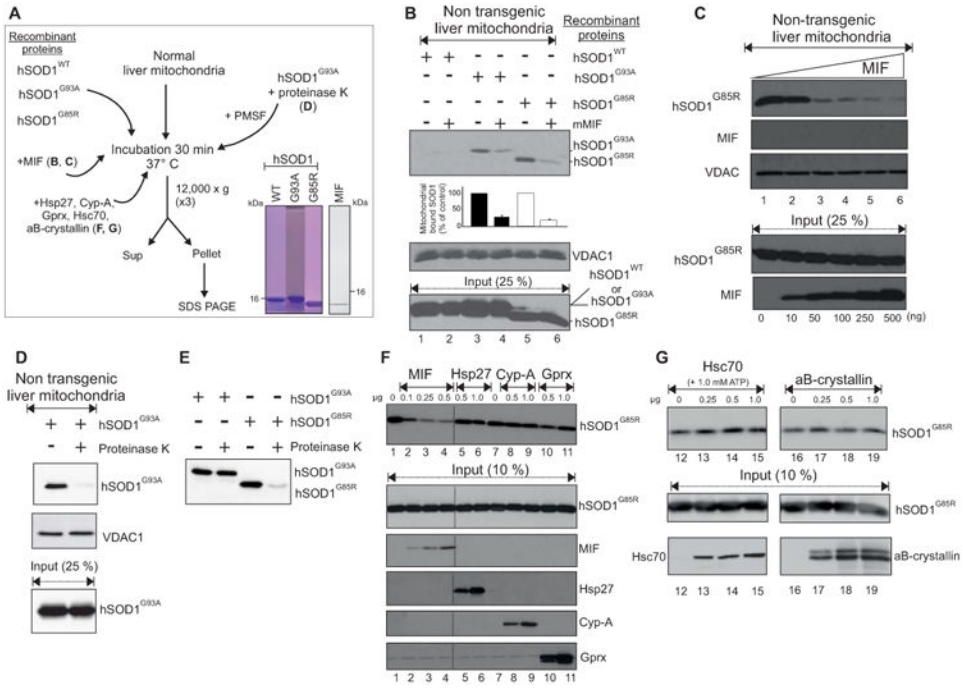

Figure 3. Recombinant MIF inhibits association of mutant SOD1 with mitochondria in a dose dependent manner

(**A**) Schematic of a protocol to test if purified recombinant MIF inhibits association of recombinant SOD1^{G85R} or SOD1^{G93A} with normal liver mitochondria. (Lower right) Coomassie stained SDS polyacrylamide gel analysis of recombinant SOD1 and MIF. (**B**) Immunoblotting of mitochondria recovered from the protocol in (**A**) and assayed for MIF-dependent inhibition of association of either SOD1^{G85R} or SOD1^{G93A} when co-incubated with non-transgenic liver mitochondria. Immunoblotting for VDAC1 was used to verify amount of mitochondria added/recovered. (**C**) Immunoblot assay as in (**A**) for dose-dependent inhibition by recombinant MIF of mutant SOD1^{G85R} binding to non-transgenic liver mitochondria. Immunoblotting for VDAC1 was used to determine mitochondrial recovery. Immunoblotting for MIF was used to determine the absence of MIF in the mitochondrial fraction and the increase levels of MIF in the supernatant that were used. (**D**) Immunoblotting of mitochondria recovered from the protocol in (**A**) and assayed for proteinase K-dependent inhibition of association of SOD1^{G93A} with non-transgenic liver mitochondria. Immunoblotting for VDAC1 was used to verify amount of mitochondria added/recovered. **(E)** Immunoblotting was used to determine the effect of proteinase K on recombinant SOD1^{G93A} or SOD1^{G85R}. (**F,G**) Assay patterned after protocol in (**A**) testing for whether purified **(F)** MIF, Hsp27, cyclophilin-A (Cyp-A), or glutathione peroxidase (Gprx) or **(G)** Hsc70 or aB-crystallin inhibit SOD1^{G85R} association with non-transgenic liver mitochondria. Some lanes were not loaded in the same order as shown in the figure.

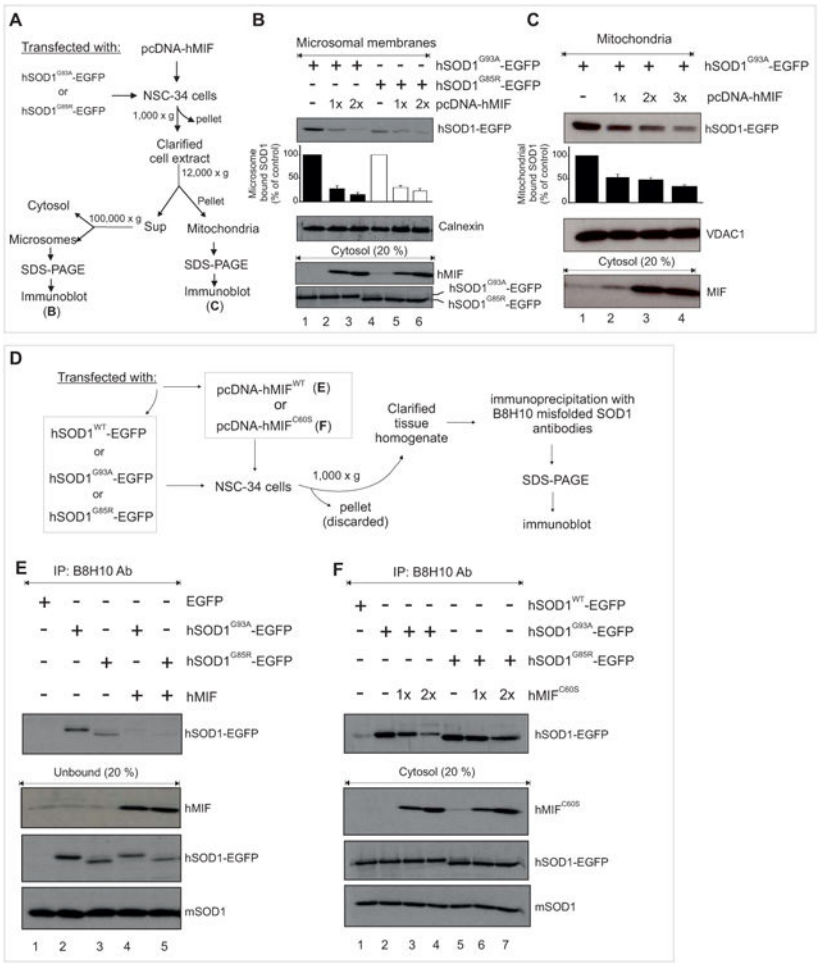

Figure 4. MIF inhibits the association of misfolded mutant SOD1 with intracellular membranes in a cell culture model of ALS

(**A**) Schematic of a protocol for assaying MIF-dependent inhibition of mutant SOD1 association *in vivo* with microsomes or mitochondria following expression of MIF and $SOD1^{G85R}$ or $SOD1^{G93A}$ in motor neuron-like NSC-34 cells. (**B, C**) Immunoblots for mutant SOD1 associated with (**B**) microsomes or (**C**) mitochondria purified from NSC-34 cells transfected to express mutant $SOD1^{G93A}$ or $SOD1^{G85R}$ and low or high levels of MIF. Parallel immunoblotting for calnexin or VDAC1 were used to verify comparable recovery of microsomes or mitochondria, respectively. Similar immunoblot analyses of the initial cytosols were used to determine initial accumulated levels or MIF and mutant SOD1. (**D**) Schematic of protocol to test if expression of MIF, with or without its thiol-oxidoreductase activity, can act *in vivo* to suppress accumulation of misfolded mutant SOD1 within NSC-34 cells. (**E,F**) MIF was expressed by transient transfection in NSC-34 motor neuron-like cells also transfected to express wild type or mutant human SOD1. Misfolded SOD1 was detected by immunoblotting of immunoprecipitates produced with the B8H10 antibody which recognizes epitopes within exon 3 that are buried in correctly folded SOD1. (**E**) Expression of wild type MIF. (**F**) Expression of MIF^{C60S} lacking thiol-oxidoreductase activity. MIF, endogenous SOD1 and EGFP-tagged wild type or mutant human SOD1 levels were determined by immunoblotting in the unbound or initial cytosol fractions.

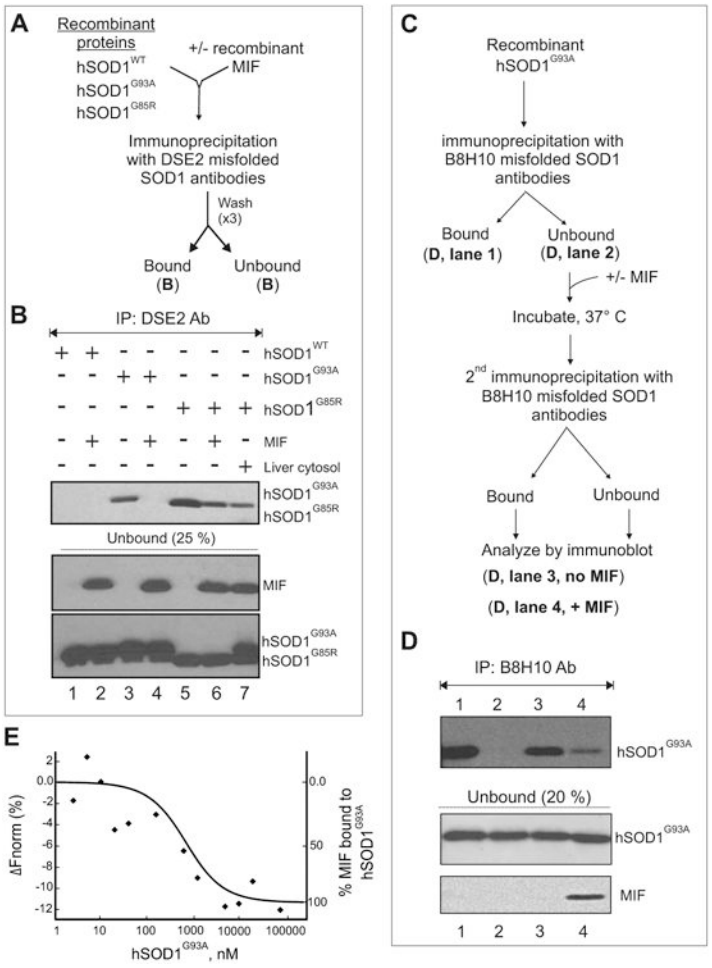

Figure 5. MIF suppresses misfolded mutant SOD1 accumulation by directly acting on it

(**A**) Protocol to determine if purified recombinant MIF suppresses accumulation of misfolded SOD1 detectable with the DSE2 antibody which recognizes an epitope in the electrostatic loop of hSOD1 (between residues 125–142) that is buried in correctly folded SOD1. (**B**) Accumulation of misfolded SOD1 was determined by immunoblotting of immunoprecipitates with the DSE2 antibody after incubation of recombinant hSOD1 wild type, hSOD1^{G93A} or hSOD1^{G85R} (4 μg) in the absence or presence of recombinant MIF (100 ng). Immunoblotting was used to determine MIF levels remaining in the unbound fraction of each immunoprecipitation assay. (**C**) Protocol to determine if purified recombinant MIF suppresses accumulation of newly formed, misfolded SOD1 detectable with B8H10 antibody for misfolded SOD1. (**D**) Misfolded SOD1 determined by immunoblotting of immunoprecipitates of recombinant hSOD1^{G93A} with the B8H10 antibody (lane 1). The unbound fraction was subjected to a second immunoprecipitation performed immediately (lane 2) or after 5 h incubation in the (lane 3) absence or (lane 4) presence of recombinant MIF. Immunoblotting was also used to determine MIF levels remaining in the unbound fraction of each immunoprecipitation assay. (**E**) Assay of MIF binding to mutant SOD1. Purified MIF (200 nM) was fluorescently labeled and incubated for 20 min at room temperature with increasing concentrations (from 2.4 nM to 80 μM) of

$SOD1^{G93A}$. (Closed diamonds) Binding of MIF to $SOD1^{G93A}$ determined by microscale thermophoresis assay. (Smooth curve) Predicted binding of MIF to mutant SOD1 calculated by curve fitting with a K_d of 367 nM (see (Jerabek-Willemsen et al., 2011; Parker and Newstead, 2014; Wienken et al., 2010)).

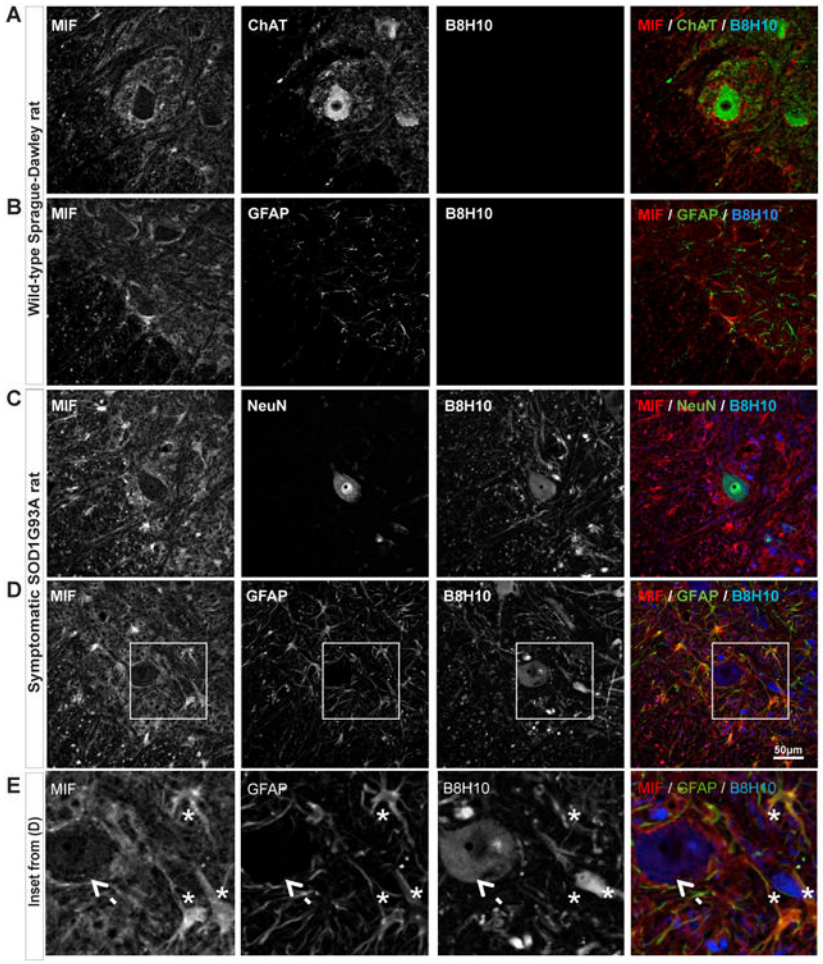

Figure 6. A low level of MIF in motor neuron cell bodies is accompanied by diffuse accumulation of misfolded SOD1 within those cell bodies just after disease onset in SOD1^{G93A} rats

(**A**) Accumulation of MIF in lumbar spinal cord of a non-transgenic rat assayed by indirect immunofluorescence with antibodies to MIF along with simultaneous identification of motor neurons (with antibodies to ChAT) and misfolded SOD1 (with antibody B8H10). **(B)** An analogous assay as in **(A)** but with astrocytes identified with an antibody to GFAP. **(C)** Accumulation of MIF in lumbar spinal cord of an early symptomatic SOD1^{G93A} rat, one week after the first spontaneous muscle fibrillation, along with simultaneous identification of motor neurons (identified by morphology, position and antibodies to NeuN) and misfolded SOD1 (with antibody B8H10). **(D)** An analogous assay as in **(C)** but with astrocytes identified with an antibody to GFAP. Scale bar, 50 µm. **(E)** Higher magnification of insets outlined in **(D)**. Arrow highlights a motor neuron lacking MIF immunostaining, and asterisks mark GFAP-positive astrocytes containing MIF.

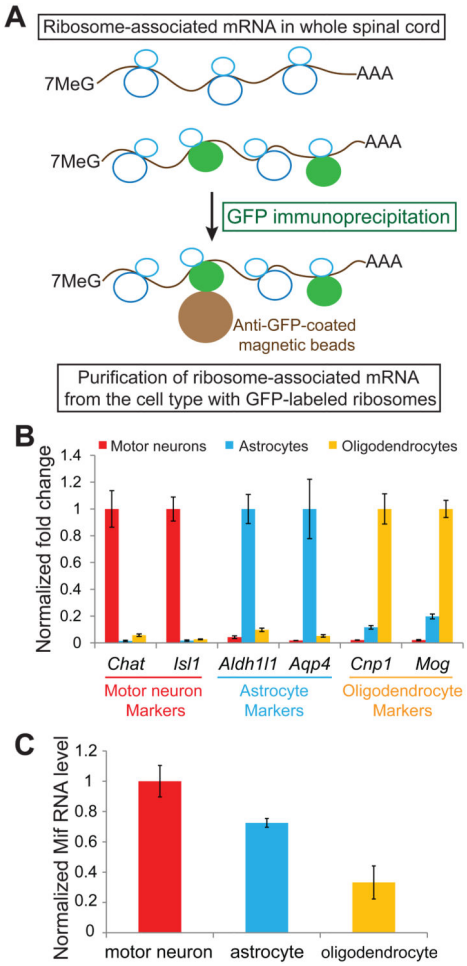

Figure 7. Translational mRNA levels of MIF in specific cell types in mouse spinal cord

(**A**) Schematic of the bacTRAP methodology for isolating cell-type specific translated mRNAs. (**B**) Relative RNA levels (assessed by qRT-PCR) of cell type-specific markers to test efficacy of polysome-associated RNA purification from motor neurons, astrocytes, and oligodendrocytes. (**C**) Relative MIF RNA level (assayed by qRT-PCR) of polysomal RNAs isolated from motor neurons, astrocytes and oligodendrocytes. Levels are normalized to Dnaja2. Error bars represent s.e.m. from 3-4 biological replicates.

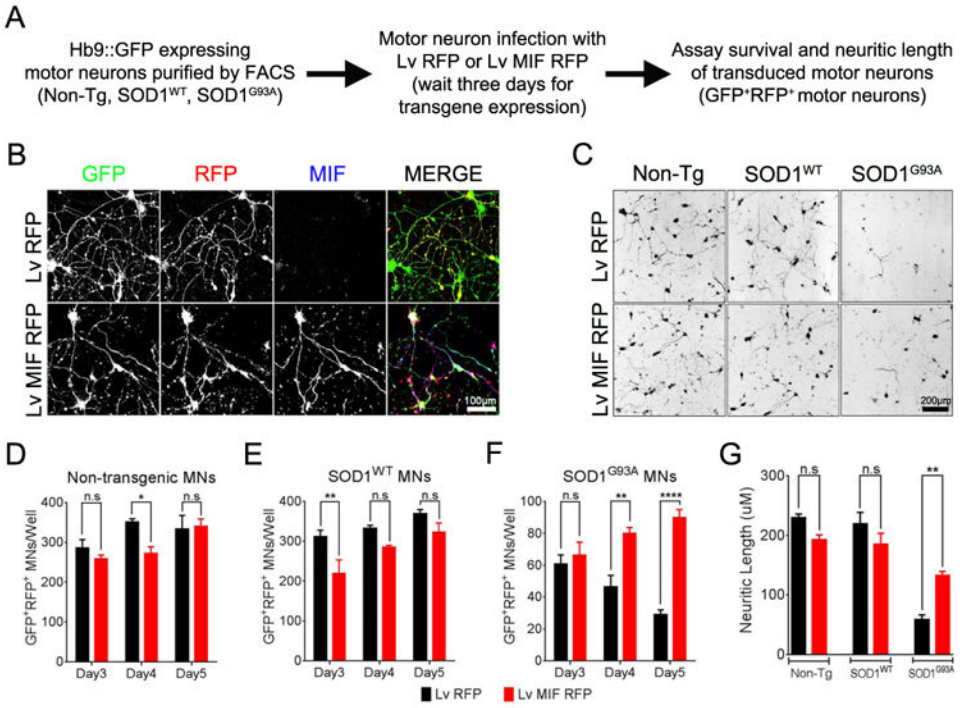

Figure 8. Increased accumulation of MIF enhances survival of primary motor neurons expressing mutant SOD1

(**A**) Protocol for generating motor neurons and assaying effects of MIF expression. **(B)** Representative images of motor neuron cultures at 96 hours post infection with LV-RFP or LV-MIF-RFP and using immunocytochemistry to reveal human MIF and RFP in motor neurons. (**C-F**) Viability of GFP+RFP+ non-transgenic, $SOD1^{WT,}$ and $SOD1^{G93A}$ motor neurons (**C**) imaged at five days or (**D-F**) quantified from images taken from three to five days after transduction with lentivirus encoding RFP or MIF and RFP. Data are representative of three independent experiments and are displayed as the mean ± s.e.m counts of triplicate wells. Two-way ANOVA was used for statistical analysis. *P< 0.05; **P< 0.01; ****P<0.0001; ns, non-significant. (**G**) Neurite length measurements quantified from images as in (**C**) taken at day five. Data shows a representative of two independent experiments and displayed as the median with range. 100 neurites per condition were included for measurements. Student's t test was used for statistical analysis. **P<0.01; ns, non-significant.